67 (2022) APPLICATIONS OF MATHEMATICS No. 6, 775–804

ON A NEW COMPUTATIONAL ALGORITHM FOR IMPACTS OF ELASTIC BODIES

Hynek Štekbauer, Ivan Němec, Rostislav Lang,
Daniel Burkart, Jiří Vala, Brno

Received May 31, 2021. Published online May 30, 2022.

Abstract. Computational modelling of contact problems is still one of the most difficult aspects of non-linear analysis in engineering mechanics. The article introduces an original efficient explicit algorithm for evaluation of impacts of bodies, satisfying the conservation of both momentum and energy exactly. The algorithm is described in its linearized 2-dimensional formulation in details, as open to numerous generalizations including 3-dimensional ones, and supplied by numerical examples obtained from its software implementation.

Keywords: computational mechanics; contact problem; finite element method; explicit time integration algorithm

MSC 2020: 74M15, 74S05, 74S20

1. Introduction

Modelling of contact is still one of the most difficult aspects of non-linear analysis. From the mechanical point of view, contact is the interaction between bodies that touch and exchange loads and energy. The global physical formulation can rely on the classical principles of continuum thermodynamics, namely on the (a) conservation of mass, (b) balance of linear and angular momentum and (c) balance of energy, corresponding to the first principle by [5], Chapter 1; the second principle is expected to be satisfied thanks to the careful choice of constitutive equations, as those from [15], Chapter 1, for various visco-elastic and visco-plastic cases.

This research has been partially supported from the project of Technology Agency CR TREND FW 03010260 (FEM Consulting Ltd. & Brno University of Technology).

DOI: 10.21136/AM.2022.0129-21

The non-linear character of contact/impact processes, even in such simple case as for a physically and geometrically linearized Kelvin visco-elastic model of 2 deformable bodies, resides in the description of behaviour of all their potential interfaces. As proposed by [41], the numerical treatment of contact problems involves the formulation of the geometry, the statement of interface laws, the integral formulation and the development of algorithms. Most computational approaches come from a simplified integral formulation of (a), (b), (c), transforming an original system of hyperbolic partial differential equations of evolutions, introduced in a weak or variational form like [42] (in the sense of its later correction [43]), supplied by the Cauchy initial conditions and the Dirichlet, Neumann, etc. boundary ones. Consequently, they preform a difference scheme for time discretization coupled with a finite element or similar technique to transform an original infinite-dimensional problem to a repeated solution of a sparse systems of linear algebraic equations.

The inequalities corresponding to interfaces, or non-linear functions covering them, can be handled by the implementation of some penalty terms, or by the addition of appropriate Lagrange multipliers, leading to the Karush-Kuhn-Tucker optimization problems; for the comparison of these approaches see [16], Part 24 of [12] and also (in the chronological order) [40], [30], [31]. The penalty approach requires the tricky choice of penalty weight and is not exact: it can be demonstrated that constraint violation is typically proportional to $1/\varepsilon$ for a positive parameter ε, whereas the violation of the energy conservation law increases, the algorithm of evaluation of approximate solution becomes unstable with increasing ε. The implementation of the Lagrange multipliers can be exact, but its disadvantage consists in the need to expand the original system of equations with the result which is not positive definite, as noticed by [34]. In this article, such computational experience is understood as a challenge to the development of an alternative approach, namely the energy motivated one, connected with the evaluation of the restitution coefficient, i.e., the ratio of the final velocity to the initial one between two objects after their collision, as introduced by [32], [2]; for its automated experimental identification cf. [18].

Another serious computational problem consists in continuation of finite element (or similar) meshes on interfaces. In the classical multi-purpose node-to-node approach by [11], [3], [37] the non-penetrating condition is applied for the opposite nodes; some one-to-one correspondence between the boundary nodes on the contacting surfaces is required. Following [47], it is an algorithmically simple and stable technique, whose advantage resides in correct treatment of contact surfaces. However, this can be guaranteed just for conforming meshes and small deformations; thus corresponding formulations are not commonly used nowadays.

The node-to-segment approach, originally derived by [13], enforces the non-penetration conditions such that the nodes of the dependent (slave) surface are prevented from penetrating the opposite independent (master) surface which results, in general, in imprecise treatment of contact surfaces, depending on the choice of the slave and the master surface. However, namely in a modified form by [48], this approach is widely used due to its simplicity, clear physical meaning and flexibility; for much more details cf. [8], [46], [45], [40]. The contact is defined between a master segment and a slave node, as illustrated for the 2-dimensional case by Fig. 1. The slave node C lies on the normal $\mathbf{n}$ (of formal unit length) of the master segment AB (of unit length, too) in the distance $\mathcal{G}_N$, the normal $\mathbf{n}$ is located in the distance $\xi|AB|$ from the node A, ξ can take values from the interval $[0, 1]$, as presented by [36]. The geometric inaccuracy can be reduced by reversing the roles of the surfaces and repeating the same process using the two-pass evaluation.

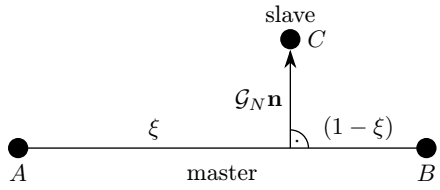

Figure 1. Geometry of the node-to-segment contact, following [36].

The alternative segment-to-segment approach by [25] applies the constraint conditions along the entire boundary in a certain weak integral sense. Consequently, the unbiased treatment of contact surfaces is sensitive on the careful choice of a special discretization scheme.

Moreover, in the case of a large number of multiple interfaces the most time consuming step in classical sequential algorithms can be the searching for potential contacts/impacts in every particular time step. This can be overcome by using selected results from the graph theory and implementation of a distributed computing platform, as discussed by [26]. This prefers the choice of explicit solvers of time-discretized problems, like the special (nearly) central difference scheme by [12], Part 24, corresponding to [4], Chapter 9.2, implemented namely in the LS-DYNA software package for multi-physics simulations, although their stability and convergence properties, namely with non-linearities from various sources, can be even worse than those induced by the classical Courant-Friedrichs-Lévy stability criterion by [7], revisited by [29], [1]. However, this is a subject of a recent intensive discussion, as evident e.g. from the substantial generalization of this scheme by [20], containing 2 additional real parameters, forcing unconditional stability for (at least) linear elastic problems, at the cost of insertion of certain more expensive implicit steps.

Unlike the extensive overview of contact/impact problems for structural dynamics as [49], [19], covering a wide class of problems in both theory and applications, the aim of this article, whose basic ideas refer to the brief conference paper [35], is much more specialized: to demonstrate a new computational algorithm for impacts of elastic bodies on a rather simple benchmark problem, open to useful generalizations, motivated by practical problems of engineering structural dynamics. Thus, in Section 2 we shall start with the physical conservation laws, directed to the formulation of a model problem (Section 2.1), including the sketch of its formal verification (Section 2.2), and continue with the discussion on stability of a computational scheme compatible with [12], Part 24 (Appendix A). This will create a basis for the detailed design and implementation of the announced original effective computational algorithm in Section 3, correct in the sense of exact validity of conservation laws even in their discrete forms, not only in some hypothetical limit case, unattached in practical calculations. The detailed description of the algorithm oriented to 2-dimensional numerical examples in Section 4 will be presented for simplicity; fortunately, their 3-dimensional generalization is rather straightforward, being prepared for another paper with the accent to more realistic engineering simulations.

2. Notations and preliminaries

Starting with the overview of classical principles of continuum thermodynamics, restricted to adiabatic processes (no heat transfer occurs), necessary for the considerations of Section 3, we come to their mathematical description in the Bochner-Sobolev spaces of abstract functions, mapping certain time interval $\mathcal{I} = [0, \tau]$ of a finite length τ to a space of admissible virtual displacements $\mathcal{V}$, related to the initial geometrical configuration, to the weak formulation of a corresponding initial and boundary problem for a system of partial differential equations of evolutions and to its finite-dimensional discretization in a rather general context. This discretization enables us to develop the needed computational algorithm and its software implementation, specified in more details in Section 3.

2.1. Physical background. For the beginning, let us consider a single deformable body Ω in the 2-dimensional Euclidean space $\mathbb{R}^2$, with its Lipschitz boundary $\partial\Omega$, supplied by certain fixed system of Cartesian coordinates x_*. Such configuration refers to its initial state in the time $t = 0$; for every time $t \in \mathcal{I}$ we shall work, due to the activity of various loads, with $\Omega_t = X(\Omega, t)$, where $X(\cdot, t)$ refers to a motion of Ω onto Ω_t locally, admitting an inverse $X^{-1}(\cdot, t)$. This enables us to introduce the 2-component displacement $u(x, t) = X(x_*, t) - x_*$, as well as the corresponding velocity $v(x, t)$ as its 1st time derivative in the form $v(x, t) = \mathrm{d}X(X^{-1}(x, t), t)/\mathrm{d}t$

and the acceleration as its 2nd time derivative similarly. To simplify such notations, the following formulae will contain upper dots instead of $\partial/\partial t$ and also $(\cdot)_{,i}$ instead of $\partial(\cdot)/\partial x_i$, where i and similarly also i, j, k, l will be indices from $\{1, 2\}$, utilized in the sense of the Einstein summation rule; moreover, the Hamilton operator $\nabla = (\partial/\partial x_1, \partial/\partial x_2)$ will be needed. Let us also notice that most considerations in this article could be generalized to the 3-dimensional Euclidean space $\mathbb{R}^3$ (instead of $\mathbb{R}^2$) naturally, but this is not discussed here in details for simplicity.

In the following considerations we shall recall only selected knowledge from principles of thermodynamics needed on the instant; for much more details see [5], Chapter 1. Introducing the so-called material derivative with respect to time $v_i' = \dot{v}_i + v_{i,j} v_j$, the balance of linear momentum reads

$$\varrho v_i' = \sigma_{ij,j} + f_i, \tag{2.1}$$

where $\sigma_{ij}(x, t)$ means the Cauchy stress tensor and $f(x, t)$ refers to the prescribed body forces; this is well-known in engineering mechanics as the Cauchy equilibrium conditions. Thanks to the applied Boltzmann continuum description, the balance of angular momentum gives just the stress symmetry $\sigma_{ij} = \sigma_{ji}$. Some constitutive equation for the evaluation of σ_{ij} is needed, using the matrices of gradients ∇v_i, ∇u_i, etc.; analogously to σ_{ij} it is natural to introduce the symmetric strain, strain rate, etc. tensors as $\varepsilon_{ij}(u) = (u_{i,j} + u_{j,i})/2$, $\varepsilon_{ij}(v) = (v_{i,j} + v_{j,i})/2$.

The practical evaluation of σ_{ij}, respecting some available data from material microstructure, its proper mathematical description and reliable experimental identification of a sufficiently small number of suggested material parameters, is a separate serious problem: some researchers try to work with fractional derivatives, auxiliary differential or integro-differential equations, etc. Here we shall accept the classical parallel visco-elastic model, referenced as the Kelvin one, i.e.,

$$\sigma_{ij} = C_{ijkl}(\varepsilon_{kl}(u) + \alpha \varepsilon_{kl}(v)), \tag{2.2}$$

where $C_{ijkl} = C_{jikl} = C_{ijlk} = C_{klij}$ are (in general) 6 independent components of the 4th order stiffness tensor and α is the structural damping factor. Additional assumptions reduce the number of these material parameters: namely for isotropic materials, $C_{ijkl} = \lambda_1 \delta_{ij} \delta_{kl} + \lambda_2(\delta_{ik}\delta_{jl} + \delta_{il}\delta_{jk})$ uses only 2 so-called Lamé coefficients λ_1 and λ_2 or alternatively 2 parameters called the Young modulus $E = \lambda_1(3\lambda_1 + 2\lambda_2)/(\lambda_1 + \lambda_2)$ and the Poisson ratio $\lambda = \lambda_1/(2(\lambda_1 + \lambda_2))$; δ_{ij} here is the Kronecker symbol (returning 1 just for $i = j$, 0 otherwise). For the hypothetical case $\alpha = 0$ (no energy dissipation is allowed), (2.2) degenerates to the classical Hooke law. Let us remark that another case with the formal setting $\alpha = 1$ and missing 1st additive term in (2.2) is frequently used in computational dynamics of compressible fluids.

The balance of momentum, as well as of mass or energy, is connected with the first principle of thermodynamics. The second principle of thermodynamics can be satisfied automatically using some reasonable setting of material characteristics, namely the positive-valued α together with the positive definiteness $C_{ijkl}a_{ij}a_{kl} \geqslant C_*a_{ij}a_{ij}$, where a_{ij} and a_{kl} form arbitrary symmetric real square matrices of order 3 and C_* is a positive constant independent of them; moreover, ϱ should be positive-valued, too. Nevertheless, this may be much less transparent in the case of physical processes active on contacts between several deformable bodies, as we shall see soon.

2.2. Weak formulation. Let us consider the Cauchy initial conditions, i.e., the zero-valued $u(\cdot,0)$ and $v(\cdot,0) = v_0(\cdot)$ for some a priori prescribed initial displacement rates. All equations like (2.1) can be rewritten in their weak formulation, i.e., in the integral ones, incorporating all needed boundary conditions, thanks to the integration by parts using the Green-Ostrogradskiĭ theorem, at least in the sense of distributional derivatives. In the following formulations, μ refers to the Lebesgue measure in Ω_t, ς to the Hausdorff measure on $\partial\Omega_t$. By multiplying all additive terms of (2.1) by time-independent virtual displacement rates $\tilde{v}$ from their admissible set satisfying the homogeneous time-independent support conditions (referring to the boundary conditions of Dirichlet type) on a subset of the boundary $\partial\Omega_t$, denoted as Θ, for $\partial\Omega_t$ transformed from its reference configuration $\partial\Omega$, we obtain

$$\int_{\Omega_t} \tilde{v}_i \varrho v_i' \,\mathrm{d}\mu(x) = \int_{\Omega_t} \tilde{v}_i(\sigma_{ij,j} + f_i)\,\mathrm{d}\mu(x). \tag{2.3}$$

Thus, thanks to the integration by parts, (2.3) yields

$$\int_{\Omega_t} \varrho\tilde{v}_i v_i' \,\mathrm{d}\mu(x) + \int_{\Omega_t} \varepsilon_{ij}(\tilde{v})\sigma_{ij}\,\mathrm{d}\mu(x) = \int_{\Omega_t} \tilde{v}_i f_i\,\mathrm{d}\mu(x) + \int_{\Gamma_t} \tilde{v}_i g_i\,\mathrm{d}\varsigma(x), \tag{2.4}$$

where $g_i(x,t)$ means the components of the prescribed surface loads on the non-supported rest of $\partial\Omega_t$ (representing the boundary conditions of the Neumann type), denoted as Γ_t. Inserting (2.2) into (2.4), we receive the final formula for the calculation of v_i and u_i.

The computational evaluation of v_i and u_i from (2.4) with (2.2) is not easy because of the unceasing change of coordinates. Consequently, most formulations in engineering mechanics work with some kinds of simplifications of such equations. The frequently used approach relies on the inaccurate small-strain transcription of (2.4) onto Ω instead of Ω_t (geometrical linearization), adopting also (2.2) in the corresponding way (physical linearization). Thus, (2.4) degenerates to

$$(\tilde{v}, \varrho a) + ((\varepsilon_{ij}(\tilde{v}), \sigma)) = (\tilde{v}, f) + \langle \tilde{v}, g\rangle. \tag{2.5}$$

Using the standard notation of Lebesgue, Sobolev and Bochner-Sobolev spaces of (abstract) functions, compatible with [28], Parts 1 and 7, we can understand $(\cdot,\cdot)$ in (2.5), valid for any $t \in \mathcal{I}$, as the scalar product in $L^2(\Omega)^2$, $((\cdot,\cdot))$ as the scalar product in $L^2(\Omega)^{2\times 2}_{\rm sym}$ and $\langle\cdot,\cdot\rangle$ as the scalar product in some $L^2(\Gamma)^2$ for $\partial\Omega = \Gamma \cup \Theta$ and any $\tilde{v} \in V := \{w \in W^{1,2}(\Omega)^2 \colon w = (0,0) \text{ on } \Theta\}$. Assuming $f \in L^2(\Omega \times \mathcal{I})^2$, $g \in L^2(\Gamma \times \mathcal{I})^2$, $C \in L^\infty(\Omega)^{(2\times 2)\times(2\times 2)}_{\rm sym}$ and $\varrho, \alpha \in L^\infty(\Omega)$, the linear system of evolution (2.5) with $a = \dot{v} = \ddot{u}$ can be analysed using the method of discretization in time, as described by [27] completely, based on the convergence properties of 2 types of the Rothe sequences of approximate solutions, mapping $\mathcal{I}$ to needed function spaces, with the results $u \in W^{1,2}(\mathcal{I}, V)$, $v \in L^2(\mathcal{I}, V)$, and $a \in L^2(\Omega \times \mathcal{I})$. The undesirable effect of such simplification can be suppressed by applying some adaptive restarting strategy, controlled by the (in)acceptability of small-strain assumptions, i.e., the reset of the Cauchy initial conditions in some time steps, or even (in the extreme case) in all considered time steps.

All above presented arguments can be repeated for a union of finite number of deformable bodies, denoted by Ω again, with potential contacts. Nevertheless, in addition to Θ and Γ, $\partial\Omega$ by (2.5) must contain an additional potential contact part Λ, decomposed to a lot of separated subsets. Formally the analogue of (2.5)

$$(\tilde{v}, \varrho a) + ((\varepsilon(\tilde{v}), \sigma)) = (\tilde{v}, f) + \langle \tilde{v}, g\rangle + \langle \mathcal{D}\tilde{v}, \sigma_*\rangle_c \tag{2.6}$$

holds, where $\langle\cdot,\cdot\rangle_c$ refers to the scalar product in $L^2(\Lambda)^2$ and all components $\mathcal{D}\tilde{v}_i$ of $\mathcal{D}\tilde{v} = (\mathcal{D}\tilde{v}_1, \mathcal{D}\tilde{v}_2, \mathcal{D}\tilde{v}_3)$ mean the interface differences in values of $\tilde{v}_i$, evaluated as their traces from adjacent parts of Ω; later we shall need also the scalar product $\langle\cdot,\cdot\rangle_\nu$ in $L^2(\Lambda)$ only. The contact stress σ_* depends on $\mathcal{D}u$ and $\mathcal{D}v$. Various models describing this dependence can be found in the literature, see, e.g., (in the chronological order) [21], [9], [17], [42], [10], [33], [14], [38], [39]. For the sake of simplicity, we shall write $\sigma_* = \gamma(\mathcal{D}u, \mathcal{D}v)$. The main aim of this article is to construct a discrete counterpart of γ following from the space and time approximations of the problem, which are described below. In the case of the Hertz-Signorini-Moreau or friction contact conditions, the function γ is multi-valued and consequently (2.6) has to be replaced with a variational inequality for the problem to be defined correctly. The function γ can be single-valued, for example, if a penalization of the dynamic contact is considered, see [17], [42]. The approach suggested in this article will be compared just with the penalization method, see Section 4.

2.3. Semi-discretized and fully discretized computational schemes. A computational scheme for (2.6), supplied with an evaluation procedure for $\mathfrak{P}(\cdot,\cdot,\cdot)$, or another comparable approach, could be based on the decomposition of such hyperbolic evolutionary problem into a sequence of elliptic problems, still in certain

infinite-dimensional (although separable) function spaces. Since their analytical solution is rarely available, consequently some additional discretization in $\mathbb{R}^3$ is required, using the finite element method typically. Thus, most engineering applications work with the reverse discretization procedure. The finite element technique is able to convert (2.5) to a sparse system of linear ordinary differential equations in time, which can be solved (at least theoretically) in the analytical form, at the expense of spectral analysis of related differential operators. Such questionable advantage disappears in case (2.6), with the occurrence of the first non-negligible non-linear term.

Searching for $u_i(x,t)$, $v_i(x,t)$ and $a_i(x,t)$ satisfying (2.6), let us introduce the multiplicative Fourier decomposition

$$u_i(x,t) = \varphi_{ip}(x)u^*_{ip}(t), \quad v_i(x,t) = \varphi_{ip}(x)v^*_{ip}(t), \quad a_i(x,t) = \varphi_{ip}(x)a^*_{ip}(t) \tag{2.7}$$

with $a^*_{ip}(t) = \dot{v}^*_{ip}(t) = \ddot{u}^*_{ip}(t)$ and a priori given functions $\varphi_{ip}(x)$; p here denotes the Einstein summation index from $\{1,\dots,n\}$ and $(\varphi_{i1},\dots,\varphi_{in})$ form the basis of a subspace V_δ of finite dimension $N \leqslant 2n$ approximating V from Section 2, $\tilde{v}_i = \varphi_{iq}$ for particular $q \in \{1,\dots,n\}$, except the nodes where zero-valued $\tilde{v}_i$'s are required by the definition of V_δ. In the simplest case $V_\delta \subset V$; for more general settings (covering the so-called variational crimes) see [6], Chapter 10. In all cases, Ω is approximated by certain Ω_δ, collected from particular elements, e.g. from tetrahedra (3-simplices), where φ_{ip} can be constructed as linear functions taking the value 1 just in 1 top and the value 0 in 3 remaining ones, i.e., the linear Lagrange splines in Ω^δ. The support conditions need to be transferred from the definition of V to V_δ; δ here is usually identified with the maximal distance of 2 points of the same element over their whole collection: clearly $\delta \to 0$ with $n \to \infty$ under some geometric (semi-)regularity conditions.

Inserting (2.7) into (2.6), setting $\tilde{v}_i$ as φ_{ip} for particular $p \in \{1,\dots,n\}$, for any $t \in \mathcal{I}$ formally creating vectors $\mathbf{u}(t)$, $\mathbf{v}(t)$ and $\mathbf{a}(t)$ from all parameters $u^*_{ip}(t)$, $v^*_{ip}(t)$ and $a^*_{ip}(t)$ involved in (2.7), we can rewrite (2.6) in its semi-discretized matrix form

$$\mathbf{M}\mathbf{a}(t) + \mathbf{C}\mathbf{v}(t) + \mathbf{K}\mathbf{u}(t) = \mathbf{F}(t) + \mathbf{G}(\mathbf{u}(t),\mathbf{v}(t)). \tag{2.8}$$

Here the positive definite square sparse matrices $\mathbf{K}$, $\mathbf{C}$ and $\mathbf{M}$ of order $3n$ are well-known as the stiffness, damping and mass matrices; the much-favoured trick with lumped masses, as implemented by [42], Section 3 (taking simple functions instead of linear Lagrange splines for the 1st left-hand side additive term of (2.6)), guarantees very simple construction of $\mathbf{M}^{-1}$, too. The right-hand side of (2.8) contains $\mathbf{F}(t)$ coming from both right-hand-side additive terms of (2.6) (performing numerical integration in Ω and on Γ) and $\mathbf{G}(\mathbf{u}(t),\mathbf{v}(t))$ from its remaining right-hand-side terms (performing numerical integration on Λ, covering all non-linear contact phenomena);

we have $\mathbf{a}(t) = \dot{\mathbf{v}}(t) = \ddot{\mathbf{u}}(t)$ again. In particular, if no contact is active, $\mathbf{G}(\cdot,\cdot)$ vanishes and (2.8) can be seen, at least for relevant time step(s), as a semi-discretized version of a standard linear problem (2.5). Let us note that, thanks to integration over Ω, Γ and Λ, all additive terms on both sides of (2.8) can be understood as certain time-variable forces; the most delicate task is the evaluation of $\mathbf{G}(\mathbf{u}(t),\mathbf{v}(t))$, corresponding to all nodal contact forces generated by the last right-hand-side additive term of (2.6), implementing decomposition (2.7). In Section 3 we shall demonstrate that such evaluation can be performed using the detailed analysis of change of 3 kinds of energy on Λ, related to particular time steps, as induced by the following considerations.

The full discretization of (2.6) needs an approximate evaluation of $\mathbf{u}(t)$, $\mathbf{v}(t)$ and $\mathbf{a}(t)$ by (2.8) for $t \in \mathcal{I}$. For the simplicity of notation, motivated by the limited extent of this article, let us apply the equidistant decomposition of $\mathcal{I}$ into a finite number m of subintervals of the length $h = \tau/m$; clearly $h \to 0$ with $m \to \infty$, the generalization to subintervals of different lengths would be straightforward. Unlike implicit computational schemes, whose practical disadvantages come from the rather complicated non-linear formulation of $\mathbf{G}(\mathbf{u}(t),\mathbf{v}(t))$, the use of an explicit computational scheme forces usually some sufficiently short steps h, even in comparison with δ, as discussed in [24]. In this article we shall apply just an explicit finite difference scheme, recommended by [12] and implemented a.o. in the LS-DYNA software package, which reads

$$\mathbf{M}\mathbf{a}_s = \mathbf{F}_s + \mathbf{G}_s(\mathbf{u}_s,\mathbf{v}_s) - \mathbf{C}\mathbf{v}_{s-1/2} - \mathbf{K}\mathbf{u}_s, \tag{2.9}$$

$$\mathbf{v}_{s+1/2} = \mathbf{v}_{s-1/2} + h\mathbf{a}_s, \quad \mathbf{v}_s = (\mathbf{v}_{s-1/2} + \mathbf{v}_{s+1/2})/2, \quad \mathbf{u}_{s+1} = \mathbf{u}_s + h\mathbf{v}_{s+1/2}$$

for $s \in \{0,1,\ldots,m\}$; all a priori known values are taken at $t = sh$. Clearly $\mathbf{v}_s$ in the 1st equation (2.9) needs to be updated by a sufficient number of steps of an iterative procedure, taking $\mathbf{v}_{s-1/2}$ as the first guess of $\mathbf{v}_s$ and exploiting the 3rd equation; fortunately $\mathbf{G}_s(\mathbf{u}_s,\mathbf{v}_s)$ is zero-valued everywhere except the active contacts. The still undefined $\mathbf{v}_{-1/2}$ in the 1st formula (2.9) for $s = 0$ can be replaced by $\mathbf{v}_0$ from the 2nd Cauchy initial condition, thus $\mathbf{v}_{-1/2} = \mathbf{v}_0 - h\mathbf{a}_0/2$ formally, whereas the 1st Cauchy initial condition forces the zero-valued $\mathbf{u}_0$ only. For $s = m$, just the first three formulae (2.9) are relevant.

The pseudo-code of Algorithm 1 represents the calculation scheme of (2.9) in the explicit evaluation of displacements, velocities and accelerations of particular points of Ω_t. This scheme refers from its line 11 to the Algorithm 2 that is used for $\mathbf{G}_s(\cdot,\cdot)$ calculation as sketched by Section 3, and is allowed to handle all impact phenomena. Non-zero values of $\mathbf{G}_s(\cdot,\cdot)$ in (2.9) will consequently appear in the fully discretized model presented by Section 3 just thanks to the triple of nodal forces $\mathbf{f}_A$, $\mathbf{f}_B$, $\mathbf{f}_C$ acting

in the nodes A, B and C, for C colliding with the straight line AB (for illustration see Fig. 2). The non-trivial determination of directions and magnitudes of all such forces will be then needed.

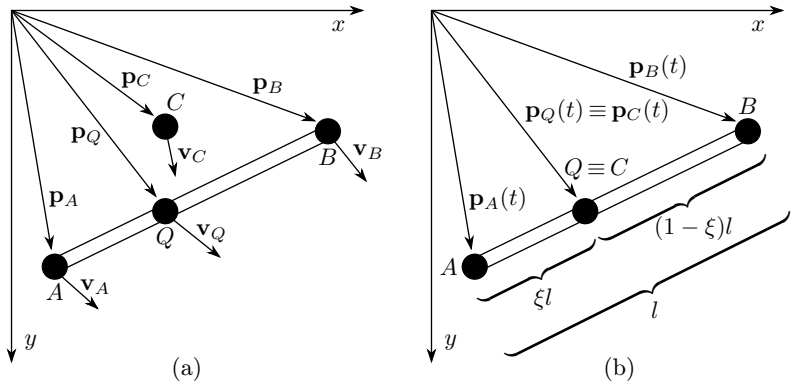

Figure 2. (a) Moving point and moving structural element before the impact. (b) Definition of the relative coordinate ξ.

Algorithm 1. Computational steps of the impact analysis.

```
1: m, τ prescribed, h = τ/m, s = 0, t_0 = 0, ε = sufficiently small value;
2: setting initial values v_0, v_{-1/2} and u_0 for Ω_0, as described in the discussion
   under (2.9);
3: while t_s ⩽ τ do
4:     v*_s = infinity, v_s = v_{s-1/2};
5:     while |v*_s − v_s| ⩾ ε|v_s| do
6:         solution of the sparse system of linear algebraic equations, represented
           by the 1st formula of (2.9), to get a_s;
7:         evaluation of v_{s+1/2} by the 2nd formula of (2.9);
8:         v*_s = v_s, evaluation of v_s by the 3th formula of (2.9);
9:         searching for active contacts pairs;
10:        for each contacts pair do
11:            calculating nodal forces for current contact pair using Algorithm 2;
12:            contributing calculated nodal forces to global vector G_s;
13:        end
14:    end
15:    t_{s+1} = t_s + h;
16:    if t_{s+1} < τ then
17:        evaluation of u_{s+1} by the 4th formula of (2.9);
18:        s ← s + 1, new configuration of Ω_{t_s};
19:    end
20: end
```

The computational scheme (2.9) could be adopted for the construction of an alternative proof of solvability of (2.6) and its possible quasi-linear generalizations, together with the detailed convergence properties of the related algorithm for $h \to 0$ and $\delta \to 0$. Appendix A of this article sketches only some stability considerations, crucial for the time stepping, unlike those less transparent by [12], relying on spectral analysis.

3. Calculation of impacts of bodies

In Section 2 we have introduced the basic idea of a contact/impact simulation of elastic bodies. However, there is still a rather long way from such formulation for a benchmark problem to an effective algorithm for practical calculations. In the following considerations we shall pay attention just to the details of evaluation of contact behaviour, i.e., to details of evaluation of the last right-hand-side term of (2.6), up to technical details for the 2-dimensional problem, with surfaces represented by line segments, where particular bodies are arbitrarily moving (and rotating) in $\mathbb{R}^2$. The whole process consists of repeated solution of impacts of nodes onto plane surfaces of elements of another bodies; an impact which occurs earlier is analysed first. The related principles can be extended to $\mathbb{R}^3$ naturally, at the expense of more complicated notations and derivations of all needed formulae. In a still more general context, this can serve as a demonstration of a thorny way from physical and mathematical non-linear benchmark problems to practical engineering calculations, up to effective general purpose software development. Basic idea comes from conservation of total energy in calculated time steps. Similar approach was proposed by [44] for node-to-node contact with need of certain mesh modification strategy; this article presents a more general node-to-surface contact, where no such compatible mesh is required.

The aim of the following considerations is to come to the practical algorithm of step-by-step calculation of vectors $\mathbf{G}_s(\mathbf{u}_s, \mathbf{v}_s)$, needed in (2.9), stemming from the evaluation of $\langle \mathcal{D}\tilde{v}, \sigma_* \rangle_c$ in (2.6) with $\sigma_\star = \gamma(\mathcal{D}u, \mathcal{D}v)$. The proposed calculation of each $\mathbf{G}_s(\mathbf{u}_s, \mathbf{v}_s)$ is based on the total energy conservation principle, where total energy Π_s before, during and after the contact/impact, related to the time $t = sh$, must coincide. Therefore, the change of energy $\Delta\Pi_s (= \Pi_s - \Pi_{s-1})$, caused by contact forces in its surrounding during one time step, consisting of changes in kinetic energy $\Delta\Pi_{ks}$, potential elastic energy $\Delta\Pi_{\sigma s}$ and potential energy of position $\Delta\Pi_{ps}$, must be equal to zero, i.e., $\Delta\Pi_s = 0$. This can be applied to every contact separately, even up to particular finite elements for a selected $s \in \{0, 1, \ldots, m\}$; namely $0 = \Delta\Pi_s(\mathbf{f}_C) = \Delta\Pi_{ks}(\mathbf{f}_C) + \Delta\Pi_{\sigma s}(\mathbf{f}_C) + \Delta\Pi_{ps}(\mathbf{f}_C)$ is utilized for the required evaluation of a contact force $\mathbf{f}_C$ in a collision of bodies. All indices s in such context are omitted. Moreover,

we shall work with $t \in [-h, 0]$ instead of $t - sh$ in the rest of Section 3 for brevity. This section describes one contact pair (as sketched by Fig. 1) and its nodes A, B, C with corresponding result contact forces $\mathbf{f}_A$, $\mathbf{f}_B$ and $\mathbf{f}_C$, generating $\mathbf{G}_s$ in the sense of Algorithm 1.

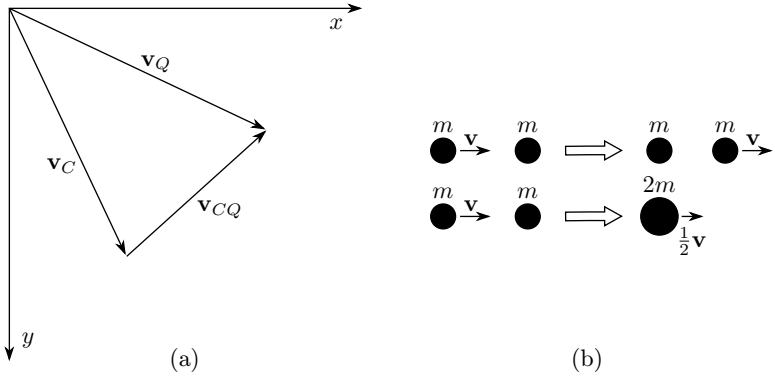

Figure 3. (a) Velocities of impacting points. (b) Impact of two idealized bodies with the same mass m: purely elastic case (upper scheme) and purely plastic one (lower scheme).

3.1. Finding the point and time of impact of moving point into moving surface. Let us assume a line segment containing 2 points A, B and another point C. Due to linearization of each time step in the explicit method, let us assume that all these points are moving with constant velocities in a fixed time step, generally each of them with different velocity. As sketched by Fig. 2 (a) and Fig. 3 (a), the initial location of the point $I \in \{A, B, C\}$ is denoted by $\mathbf{p}_I(0)$ and the velocity of the point I by $\mathbf{v}_I$. Thus, we have the general formula for positions of the points in time t:

$$\mathbf{p}_I(t) = \mathbf{p}_I(0) + \mathbf{v}_I t \quad \text{with } I \in \{A, B, C\} \text{ and } t \in [-h; 0]. \tag{3.1}$$

We want to detect whether the location of the point C will be on the line segment AB in an instant of the current time step. For this purpose, at first, we shall find out the time t in which the point C will be located on the line AB. In such configuration both vectors $\mathbf{p}_C(t) - \mathbf{p}_A(t)$ and $\mathbf{p}_B(t) - \mathbf{p}_A(t)$ are parallel, as well as the vectors perpendicular to $\mathbf{p}_C(t) - \mathbf{p}_A(t)$ and $\mathbf{p}_B(t) - \mathbf{p}_A(t)$. Let us define the mapping $\mathcal{P}$ which assigns a perpendicular vector to a given vector in $\mathbb{R}^2$. In particular, in this way, to any vector (x, y) a vector $(-y, x)$, or $(y, -x)$, is assigned. Using central dots for scalar products in $\mathbb{R}^2$, we are able to write

$$(\mathbf{p}_C(t) - \mathbf{p}_A(t)) \cdot \mathcal{P}(\mathbf{p}_B(t) - \mathbf{p}_A(t)) = 0. \tag{3.2}$$

Substituting from (3.1) into (3.2) and applying the brief notation $\mathbf{v}_{AC} = \mathbf{v}_C - \mathbf{v}_A$, $\mathbf{p}_{AC} = \mathbf{p}_C(0) - \mathbf{p}_A(0)$, $\mathbf{v}_{AB} = \mathbf{v}_B - \mathbf{v}_A$, $\mathbf{p}_{AB} = \mathbf{p}_B(0) - \mathbf{p}_A(0)$, we receive the quadratic equation $\mathcal{A}_2 t^2 + \mathcal{A}_1 t + \mathcal{A}_0 = 0$ for a variable t, whose coefficients are

$$\mathcal{A}_2 = \mathbf{v}_{AC} \cdot \mathcal{P}(\mathbf{v}_{AC}),\ \mathcal{A}_1 = \mathbf{p}_{AC} \cdot \mathcal{P}(\mathbf{v}_{AB}) + \mathbf{v}_{AC} \cdot \mathcal{P}(\mathbf{p}_{AB}),\ \mathcal{A}_0 = \mathbf{p}_{AC} \cdot \mathcal{P}(\mathbf{p}_{AB}). \tag{3.3}$$

We shall need (if possible) its real root $t_{c1,2} = \left(\pm\sqrt{\mathcal{A}_1^2 - 4\mathcal{A}_0\mathcal{A}_2} - \mathcal{A}_1\right)/(2\mathcal{A}_2)$.

Obtaining two complex conjugated roots from (3.3) means that the point C could not possibly cross the line AB in a linearized time step in the current configuration of position and velocities. We do not investigate this case anymore, as well as any degenerated case with $\mathcal{A}_2 = \mathcal{A}_1 = 0$. To obtain the time of the contact and the space coordinates of nodes, the roots t_{c1} and t_{c2} must be real; both roots must be investigated because only one of them has a physical meaning. The roots represent time of possible contact of the line AB and the point C. We investigate whether the time of the contact belongs to the elapsed time step h. It follows that if $t_c > 0$, then the contact has yet to occur; otherwise the contact has already occurred. If the contact occurred in the elapsed time step h, for the time t_c, $-h \leqslant t_c \leqslant 0$ holds. If both of the roots satisfy the condition, the lower one $t_{c1} \leqslant t_{c2}$ is valid, the later contact could not occur.

If t_c lies in the needed interval and the line segment AB is not degenerated, then we must check whether the point C lies within this line segment. Let Q be (in the general context) the result of projection of the point C to the line AB; Fig. 2 (b) shows the case where both points C and Q coincide. Since the point Q lies always on the line AB, we have

$$\mathbf{p}_Q(t) = \mathbf{p}_A(t) + \hat{t}(\mathbf{p}_B(t) - \mathbf{p}_A(t)) \tag{3.4}$$

for a parameter $\hat{t}$ (as a function of t, too). Seemingly the point Q (so also the point C) is contained in the line segment AB if $0 \leqslant \hat{t} \leqslant 1$; however, when deriving the time of the collision, $C \equiv Q$ is not supposed yet, but (in the opposite case) the pair of lines CQ and AB must be perpendicular, i.e.,

$$(\mathbf{p}_C(t) - \mathbf{p}_Q(t)) \cdot (\mathbf{p}_B(t) - \mathbf{p}_A(t)) = 0. \tag{3.5}$$

Thus, (3.4) and (3.5) result in

$$\hat{t} = \frac{(\mathbf{p}_C(t) - \mathbf{p}_A(t)) \cdot (\mathbf{p}_B(t) - \mathbf{p}_A(t))}{(\mathbf{p}_B(t) - \mathbf{p}_A(t)) \cdot (\mathbf{p}_B(t) - \mathbf{p}_A(t))}. \tag{3.6}$$

The location of all points A, B, C, Q (given by $\mathbf{p}_A$, $\mathbf{p}_B$, $\mathbf{p}_C$, $\mathbf{p}_Q$) in the time of the impact t_c can be obtained easily, substituting $t = t_c$ into (3.1) and (3.4) with $\hat{t}$ taken from (3.6).

3.2. Determination of the direction of impact forces $\mathbf{e}_C$. At first, let us assume the impact of two mass points in the one-dimensional case. It is needed to determine the velocities of the mass points after the impact. The solution must satisfy the laws of conservation of energy and momentum, as introduced (in much more general context) in Section 2; 2 equations for 2 velocities enable us to solve the problem, cf. Fig. 3 (b).

Let us notice that the formulation of such problem in $\mathbb{R}^3$ requires to determine 6 unknown components of 2 velocity vectors, but only 4 equations from the conservation laws are available: 3 of them obtained from conservation of (translational) momentum and 1 from conservation of energy. In $\mathbb{R}^2$ it is needed to determine 4 unknown components of 2 velocity vectors while having only 3 equations at disposal. Thus, an infinite number of solutions satisfying these conservation laws exists. To obtain the correct and unique solution, a suitable additional hypothesis must be adopted, concerning the determination of the direction of the velocity of at least 1 of 2 colliding mass points. The impact of 2 infinitesimal mass points is not practically important and can be regarded as an exceptional case of the general case of the impact of a mass point on a surface.

Let us consider 2 limit cases. At first, let us assume that the friction is absolute and no slip between the mass point and the surface during the impact occurs. Then the mass points C and Q will bounce in the same relative direction $\mathbf{v}_{CQ} = \mathbf{v}_Q - \mathbf{v}_C$ as before the impact, but moving to the opposite sides. The impact force $\mathbf{f}_Q^a$ acting on the point Q will have the same direction as the relative velocity $\mathbf{v}_{CQ}(t)$, whereas the impact force $\mathbf{f}_C^a$ acting on the point C has the opposite direction. Thus, it is easy to define, applying the Euclidean norm $|\cdot|$ in $\mathbb{R}^2$, also the unit vector $\mathbf{e}_Q^a = \mathbf{f}_Q^a/|\mathbf{f}_Q^a| = \mathbf{v}_{CQ}/|\mathbf{v}_{CQ}|$. As the second limit case, let us suppose that there is zero friction between the impacting bodies. In this case the force between the mass point and the surface must be normal to the surface in the point of the impact; the angles between the normal to the surface and the velocities of the mass point must be the same and these 2 vectors must be oriented symmetrically to the normal of the surface. Let us introduce the vector $\mathbf{n}_{AB}$ normal to the line AB, which is the direction of the contact force in the limit case of zero friction; thus (for an arbitrary t again) $\mathbf{n}_{AB} = \mathcal{P}(p_B(t) - p_A(t))$.

Between the impacting points C and Q an impact force must act in the sense of the classical 3rd Newton law. The directions of the impact forces $\mathbf{f}_Q^z$ and $\mathbf{f}_C^z$ acting at the points Q and C can be determined as $\mathbf{e}_Q^z = \mathbf{f}_Q^z/|\mathbf{f}_Q^z| = \mathbf{n}_Q/|\mathbf{n}_Q|$ using the simple rule

$$\begin{aligned} &\mathbf{n}_{AB} \cdot \mathbf{v}_{CQ}(t) \geqslant 0 \Rightarrow \mathbf{n}_Q = \mathbf{n}_{AB}, \\ &\mathbf{n}_{AB} \cdot \mathbf{v}_{CQ}(t) \leqslant 0 \Rightarrow \mathbf{n}_Q = -\mathbf{n}_{AB}. \end{aligned} \tag{3.7}$$

In real engineering simulations, the friction between the surface, analysed by (3.7), is rarely none or absolute; something between both limit cases occurs. Therefore, it is reasonable for the angle of the relative velocity vectors to be taken as a linear combination of both limit cases. For this purpose it can be useful to introduce the dimensionless weight coefficient β with values between 0 and 1 and to express $\mathbf{e}_Q = \mathbf{f}_Q/|\mathbf{f}_Q|$, where $\mathbf{f}_Q = \beta\mathbf{e}_Q^a + (1-\beta)\mathbf{e}_Q^z$. The unit impact force, acting in the point C in the opposite direction, can be then taken as $-\mathbf{e}_Q$. The value of β can be identified experimentally for specific materials and surfaces. Such friction without energy dissipation, used in this paper exclusively, can be seen as an alternative to other friction models, e.g. to the classical Coulomb model, utilized in [10], its velocity-driven variant by [42], or the LuGre and Dahl models, analyzed by [23]; for even more approaches to evaluation of friction cf. [22].

3.3. Evaluation of impact of mass point into a finite element surface. In most software applications a stiffness of impact in the defined direction of the force between two impacted bodies is considered as a crucial step for the penalty method. The disadvantage of this method is a certain randomness in calculation of the force between the impacted bodies. To guarantee that the bouncing force satisfies the conservation of energy well enough, it is necessary to ensure that the whole process of braking and accelerating of the impacted bodies lasts at least 5 or 6 time steps (by mostly empiric observations) in all explicit evaluations, as sketched by Section 2. This can be seen as a motivation for the development of quite another approach.

Such approach can come from the careful evaluation of the contact force $\mathbf{f}_{CQ}$ acting at the impacting points. The force $\mathbf{f}_{CQ}$ can be seen as an internal force in the case of contact always pressure with zero resultant, representing 2 opposite forces $\mathbf{f}_C$ and $\mathbf{f}_Q$ acting on the impacted bodies, in particular at the points of the impact C and Q, respectively in the sense of the 3rd Newton law. Therefore, the force $\mathbf{f}_Q$ acting at the point Q is opposite to the force $\mathbf{f}_C$ acting at the point C. In our configuration, $\mathbf{f}_Q = \mathbf{f}_{CQ}$ and $\mathbf{f}_C = -\mathbf{f}_{CQ}$. The direction of this force depends on the vector of the velocity of the point C related to the element AB and on the magnitude of friction between the impacting bodies; its determination has been described above. For the determination of the magnitude of the force $\mathbf{f}_{CQ}$, a fictitious time step $h_C = h$, admitting only the loading by the unknown force $\mathbf{f}_{CQ}$, is introduced now. This special time step h_C is not real and serves only for calculation of such a magnitude of the contact force acting within one time step to fulfil the energy conservation during the collision exactly. Increments of time, positions, velocities and forces calculated in the fictitious time step are not added to the present state. To the next real time step, the nodal forces equivalent to the contact forces calculated in the fictitious time step

are added to the present nodal forces. It is necessary to determine its magnitude so that in one time step h_C such acceleration of 3 points A, B and C occurs that their velocities and positions at the end of this time step provide the same total energy, possibly decreased by the energy dissipation during the impact.

3.3.1. Preparatory considerations. Let us consider discretized (lumped) masses m_I assigned to particular points $I \in \{A, B, C, Q\}$; they are just the elements of the diagonalized matrix M from (2.8), as well as the discretized nodal masses in Section 4. The forces $\mathbf{f}_C$ and $\mathbf{f}_Q$ cause at the point C and Q the accelerations $\mathbf{a}_C = \mathbf{f}_C/m_C$, $\mathbf{a}_Q = \mathbf{f}_Q/m_Q = -\mathbf{f}_C/m_Q$, respectively; the corresponding increments of velocity at the end of the time step are $\Delta\mathbf{v}_C = \mathbf{a}_C h_C$, $\Delta\mathbf{v}_Q = \mathbf{a}_Q h_C$. Regarding the fact that the point Q is not a regular node in the analysed system but a common point on the line segment AB, it is necessary to substitute the force $\mathbf{f}_Q$ with 2 equivalent forces $\mathbf{f}_A$ and $\mathbf{f}_B$, applied respectively at the points A and B in the sense of equivalence of translational and rotational momentum. The equivalence of the translational momentum is expressed by the relation

$$\Delta\mathbf{v}_Q m_Q = \Delta\mathbf{v}_A m_A + \Delta\mathbf{v}_B m_B. \tag{3.8}$$

The equivalence of the rotational momentum, accounting for zero rotational momentum of the mass m_Q to the point Q is expressed by the relation

$$\Delta\mathbf{v}_A m_A \xi - \Delta\mathbf{v}_B m_B (1-\xi) = 0, \tag{3.9}$$

as presented by Fig. 2 (b). Here $\xi = x_t/l$ and $1-\xi = (l-x_t)/l$ are the relative distances of the point Q from the points A and B. While the point A lies at the zero origin of the axis x_t, the point B lies at the place $x_t = l$ and the point Q at the place x_t.

From (3.8) and (3.9), supplied by the obvious relation $m_Q = m_A + m_B$, we come to the evaluation formulae for the increment of velocities $\Delta\mathbf{v}_A$ and $\Delta\mathbf{v}_B$, at the points A and B, respectively, analogous to $\Delta\mathbf{v}_C$ presented above, in the form

$$\begin{aligned} \Delta\mathbf{v}_A &= \Delta\mathbf{v}_Q \frac{m_A + m_B}{m_A}(1-\xi) = -\frac{\mathbf{f}_C}{m_A}(1-\xi)h_C, \\ \Delta\mathbf{v}_B &= \Delta\mathbf{v}_Q \frac{m_A + m_B}{m_B}\xi = -\frac{\mathbf{f}_C}{m_B}h_C, \quad \Delta\mathbf{v}_C = \frac{\mathbf{f}_C}{m_C}h_C. \end{aligned} \tag{3.10}$$

Consequently, we are able to calculate also the resulting velocities of the points A, B and C at the end of the fictitious time step $\mathbf{v}_I^* = \mathbf{v}_I + \Delta\mathbf{v}_I$ with $I \in \{A, B, C\}$, as well as the change of positions of the same points $\Delta\mathbf{u}_I = \mathbf{v}_I h_C$ and the resulting positions $\mathbf{u}_I^* = \mathbf{u}_I + v_I^* h_C$.

No positions of the remaining nodes of the structure change in this fictitious time step. In the case that some deformation parameters at the points A, B and C are supported, it is necessary to ensure that their increments of velocities and positions will be zero-valued. Calculation of all changes of energy caused by the force $\mathbf{f}_{CQ}$ in the fictitious time step h_C consists of three steps: of those i) of the kinetic energy $\Delta\Pi_k$, ii) of the elastic potential energy of elements $\Delta\Pi_\sigma$, iii) of the potential energy corresponding to particular positions $\Delta\Pi_p$. The corresponding notation Π_J and $\Pi_J^* = \Pi_J + \Delta\Pi_J$ with the symbolic indices $J \in \{k, \sigma, p\}$ for the energy of various kinds before and after the impact will be applied, too.

During the fictitious time step, only the velocities of the nodes A, B and C will change. In the following formulae, based on the change of 3 various kinds of energy, we shall apply the Einstein summation index $I \in \{A, B, C\}$.

3.3.2. Change of kinetic energy $\Delta\Pi_k$. For the kinetic energy, whose change is controlled by $\mathbf{f}_C$, thanks to (3.10) we have

$$
\begin{aligned}
(3.11)\quad \Pi_k &= \frac{1}{2} m_I \mathbf{v}_I \cdot \mathbf{v}_I, \quad \Pi_k^* = \frac{1}{2} m_I \mathbf{v}_I^* \cdot \mathbf{v}_I^*, \\
\Delta\Pi_k &= \Pi_k^* - \Pi_k = \frac{1}{2} m_I \mathbf{v}_I^* \cdot \mathbf{v}_I^* - \frac{1}{2} m_I \mathbf{v}_I \cdot \mathbf{v}_I = \frac{1}{2} m_I (2\mathbf{v}_I \cdot \Delta\mathbf{v}_I + \Delta\mathbf{v}_I \cdot \Delta\mathbf{v}_I) \\
&= \frac{1}{2} m_A \Big(-\frac{2\mathbf{f}_C \cdot \mathbf{v}_A}{m_A} (1-\xi) + \frac{\mathbf{f}_C \cdot \mathbf{f}_C}{m_A^2} (1-\xi)^2 {h_C}^2 \Big) \\
&\quad + \frac{1}{2} m_B \Big(-\frac{2\mathbf{f}_C \cdot \mathbf{v}_B}{m_B} \xi + \frac{\mathbf{f}_C \cdot \mathbf{f}_C}{m_B^2} \xi^2 {h_C}^2 \Big) + \frac{1}{2} m_C \Big(\frac{2\mathbf{f}_C \cdot \mathbf{v}_C}{m_C} + \frac{\mathbf{f}_C \cdot \mathbf{f}_C}{m_C^2} {h_C}^2 \Big) \\
&= -\mathbf{v}_A \cdot \mathbf{f}_C (1-\xi) h_C + \frac{\mathbf{f}_C \cdot \mathbf{f}_C}{2m_A} (1-\xi)^2 {h_C}^2 \\
&\quad - \mathbf{v}_B \cdot \mathbf{f}_C \xi h_C + \frac{\mathbf{f}_C \cdot \mathbf{f}_C}{2m_B} \xi^2 {h_C}^2 + \mathbf{v}_C \cdot \mathbf{f}_C h_C + \frac{\mathbf{f}_C \cdot \mathbf{f}_C}{2m_C} {h_C}^2.
\end{aligned}
$$

3.3.3. Change of potential elastic energy $\Delta\Pi_\sigma$. With regards to the fact that only positions of the points A, B and C are allowed to change in the given fictitious time step, only the elastic potential energy of the elements including those nodes may change. In our case we limit ourselves to linear truss rods. Let η refer to particular element indices, being considered as the Einstein summation index again, with admissible integer values from 1 to the total number of such elements. For any η let $\mathcal{L}_{0\eta}$ be the original element length and $\mathcal{L}_\eta$ its length at the beginning of the fictitious time step, i.e., in the time of contact of the points C and Q; moreover $\Delta\mathcal{L}_\eta := \mathcal{L}_\eta - \mathcal{L}_{0\eta}$, being the total element length change at the end of the fictitious time step. At the end of the time step, the length $\mathcal{L}_\eta$ from its beginning is modified to $\mathcal{L}_\eta^*$; $\Delta\mathcal{L}_\eta^* := \mathcal{L}_\eta^* - \mathcal{L}_{0\eta}$ being the total element length change at the beginning of the fictitious time step analogously. For example, let us assume that the line

segment AB is a representation of a truss element with the cross section area $\mathcal{A}_\eta$ and its Young modulus E (the same everywhere). Thus, we are ready to express the elastic potential energy as

$$\Pi_\sigma = \frac{1}{2} E\mathcal{A}_\eta \Big(\frac{\mathcal{L}_\eta - \mathcal{L}_{0\eta}}{\mathcal{L}_{0\eta}}\Big)^2 = \frac{E\mathcal{A}_\eta}{2\mathcal{L}_{0\eta}^2}\Delta\mathcal{L}_\eta^2,$$
$$\Pi_\sigma^* = \frac{1}{2} E\mathcal{A}_\eta \Big(\frac{\mathcal{L}_\eta^* - \mathcal{L}_{0\eta}}{\mathcal{L}_\eta^*}\Big)^2 = \frac{E\mathcal{A}_\eta}{2\mathcal{L}_{0\eta}^2}\Delta\mathcal{L}_\eta^{*2},$$
$$\Delta\Pi_\sigma = \Pi_\sigma^* - \Pi_\sigma = \frac{E\mathcal{A}_\eta}{2\mathcal{L}_{0\eta}^2}(2\Delta\mathcal{L}_\eta + \Delta\mathcal{L}_\eta^*)\Delta\mathcal{L}_\eta^*. \tag{3.12}$$

3.3.4. Change of potential energy of position $\Delta\Pi_p$. To utilize the last equation of (3.12) as the computational formula, 2 occurrences of particular $\Delta\mathcal{L}_\eta^*$ on its right-hand side need the proper evaluation. No exact effective method is available, thus we apply the linearized equations for the change of element lengths, based on the projections of member ends of displacement increments into the member axis, in the form

$$\Delta\mathcal{L}_\eta^* = \mathcal{L}_{0\eta}(\Delta\mathbf{u}_\mathcal{N} - \Delta\mathbf{u}_\mathcal{M}) = \mathcal{L}_{0\eta}\Big(\mathbf{v}_\mathcal{N} h_C + \frac{\mathbf{f}_C \vartheta_\mathcal{N}}{2m_\mathcal{N}} {h_C}^2 - \mathbf{v}_\mathcal{M} h_C - \frac{\mathbf{f}_C \vartheta_\mathcal{M}}{2m_\mathcal{M}} {h_C}^2\Big) \tag{3.13}$$

for every η (without any summation here). The nodal positions increments are expressed in terms of nodal velocities and accelerations in the given time step.

In (3.13), $\vartheta_\mathcal{M}$ and $\vartheta_\mathcal{N}$ represent the multiplicative weight coefficients applied to the force $\mathbf{f}_Q - \mathbf{f}_C$ being multiplied at pertinent element ends. Therefore, $\vartheta\mathbf{f}_C$ can be interpreted as the increment of the nodal force in the fictitious time step from the contact force $\mathbf{f}_C$. Consequently, $\vartheta_A = -(1-\xi)$, $\vartheta_B = -\xi$, $\vartheta_C = 1$ and $\vartheta = 0$ in all remaining nodes.

Finally, the change of the potential energy, thanks to the fact that only 3 points A, B and C are loaded by some non-zero forces $\mathbf{f}_{QC}$, can be calculated as

$$\Delta\mathbf{u}_A = -\frac{\mathbf{f}_C}{m_A}(1-\xi){h_C}^2,$$
$$\Delta\mathbf{u}_B = -\frac{\mathbf{f}_C}{m_B}\xi{h_C}^2, \quad \Delta\mathbf{u}_C = \frac{\mathbf{f}_C}{m_C}{h_C}^2,$$
$$\Delta\Pi_p = -\Delta\mathbf{u}_\eta \mathbf{f}_\eta^{\mathrm{ext}} = \frac{\mathbf{f}_C \cdot \mathbf{f}_A^{\mathrm{ext}}}{m_A}(1-\xi){h_C}^2 + \frac{\mathbf{f}_C \cdot \mathbf{f}_B^{\mathrm{ext}}}{m_B}\xi{h_C}^2 - \frac{\mathbf{f}_C \cdot \mathbf{f}_C^{\mathrm{ext}}}{m_C}{h_C}^2, \tag{3.14}$$

where all upper indices in $\mathbf{f}_A^{\mathrm{ext}}$, $\mathbf{f}_B^{\mathrm{ext}}$ and $\mathbf{f}_C^{\mathrm{ext}}$ refer to pertinent external forces. Notice that the velocities at the beginning of the fictitious time step are not taken into account because in the fictitious time step we investigate only the influence of the contact force to a change of the pertinent nodes positions $\Delta\mathbf{u}_\eta$.

3.3.5. Calculation of the magnitude of impact nodal force $\mathbf{f}_C$ from total energy change $\Delta\Pi = \Delta\Pi_k(\mathbf{f}_C) + \Delta\Pi_\sigma(\mathbf{f}_C) + \Delta\Pi_p(\mathbf{f}_C) = 0$. The change of the total energy Π to its new value Π^* can be presented as $\Pi^* - \Pi = \Delta\Pi = \Delta\Pi_k + \Delta\Pi_\sigma + \Delta\Pi_p + E_q$, where E_q refers to the dissipatied energy during the impact, which for an impact of elastic bodies is equal to zero. If any non-negligible plastic or damage effects occur, their influence must be estimated by an independent calculation, and for the presented algorithms they can be regarded as given.

All energy contributions are functions of the contact force

$$\mathbf{f}_C = |\mathbf{f}_C|\mathbf{e}_C. \tag{3.15}$$

Thus, the energy change during the impact $\Delta\Pi$ can be seen as a function of one scalar variable, interpretable as the magnitude of the contact force $|\mathbf{f}_C|$, and of a duration of the fictitious time step h_C. Then the relation expressing the energy conservation reads

$$\Delta\Pi(|\mathbf{f}_C|, h_C) = \Delta\Pi_k(|\mathbf{f}_C|, h_C) + \Delta\Pi_\sigma(|\mathbf{f}_C|, h_C) + \Delta\Pi_p(|\mathbf{f}_C|, h_C) = -E_q. \tag{3.16}$$

For all presented examples in this paper we assume $E_q = 0$. The magnitude of the impulse of the contact force must satisfy (3.16). When the magnitude of the fictitious time step (i.e., duration of acting of the contact force, $h_C = h$) is chosen, the magnitude of the contact force can be calculated.

The formulae for calculation of the kinetic energy and the potential energy of position contain only linear and quadratic terms with unknown $|\mathbf{f}_C|$. Only the evaluation of the elastic potential energy cannot avoid the square root of $|\mathbf{f}_C|$ when calculating the element lengths at the end of the fictitious time step.

Therefore, to obtain the quadratic equation for $|\mathbf{f}_C|$ in its closed form, it is needed to calculate the change of the line segment length in a linearized form. Then the calculation would lead to a solution of a certain quadratic equation without an absolute term, which vanishes when detracting the energy at the beginning of the time step from the energy at the end of the time step. Only the positive root of such equation has the physical sense.

The crucial step consists in the linearization of (3.13). The unknown variable must be evaluated using an iterative process, e.g. based on the classical Newton method, fortunately (not to debase effective computations) only as the one-dimensional method of tangents. For the first iteration, the root of the quadratic equation obtained from exact change of the kinetic and the potential energy of the position can be used as a starting value of the increment of the energy. The linear and the quadratic coefficients of the quadratic equation are obtained as a sum of all

coefficients of linear and quadratic terms of the required force magnitude $|\mathbf{f}_C|$; in the case of potential energy of the position, the corresponding term is even only linear. After rather long calculations (whose details are left to the curious reader) we come to the final result

$$\mathbf{e}_C|\mathbf{f}_C|\cdot\Big[\mathbf{e}_C|\mathbf{f}_C|\Big(\frac{(1-\xi)^2{h_C}^2}{2m_A}+\frac{\xi^2{h_C}^2}{2m_B}+\frac{{h_C}^2}{2m_C}\Big) + \mathbf{v}_C-\mathbf{v}_A(1-\xi)-\mathbf{v}_B\xi+\frac{\mathbf{f}_A^{\mathrm{ext}}}{m_A}(1-\xi)h_C+\frac{\mathbf{f}_B^{\mathrm{ext}}}{m_B}\xi h_C-\frac{\mathbf{f}_C^{\mathrm{ext}}}{m_C}h_C\Big]=0. \tag{3.17}$$

Since the root $|\mathbf{f}_C|=0$ gives no physically reasonable result, the 2nd part of (3.17) provides always an explicit formula for the evaluation $|\mathbf{f}_C|$.

Thanks to (3.15), the 1st derivative $(\Delta\Pi)'$ of $\Delta\Pi=\Delta\Pi_k+\Delta\Pi_\sigma+\Delta\Pi_p$ with respect to $|\mathbf{f}_C|$ can be now determined by (3.11), (3.12), including (3.13), and (3.14) analytically. Consequently, $\Delta\Pi=0$ can be achieved using its above derived estimate of $|\mathbf{f}_C|_0$ and the iterative procedure

$$|\mathbf{f}_C|_{\zeta+1}=|\mathbf{f}_C|_\zeta-\Delta\Pi(|\mathbf{f}_C|_\zeta)/(\Delta\Pi)'(|\mathbf{f}_C|_\zeta), \tag{3.18}$$

where $\zeta\in\{0,1,2,\ldots\}$ is the iteration step number. Moreover, we can take

$$\Delta\mathbf{v}_A=\frac{\mathbf{f}_A}{m_A}h_C,\quad \Delta\mathbf{v}_B=\frac{\mathbf{f}_B}{m_B}h_C. \tag{3.19}$$

Substituting (3.19) into (3.10), we obtain

$$\mathbf{f}_A=\Delta\mathbf{v}_A\frac{m_A}{h_C}=-\mathbf{f}_C(1-\xi),\quad \mathbf{f}_B=\Delta\mathbf{v}_B\frac{m_B}{h_C}=-\mathbf{f}_C\xi. \tag{3.20}$$

Lastly, (3.15) and (3.20) complete the evaluation of all required forces at the points A, B and C. Several collisions indicated in the same time step can be treated simultaneously if they do not influence the forces at the same node; otherwise only the collision occurring first is considered in such time step. In the next time step, all conditions are checked again and handled if necessary.

3.4. Satisfying conservation laws. An important characteristic of each computational algorithm in engineering mechanics is its respecting of conservation of mass, momentum and energy just at the discretized level, not only in some hypothetical limit sense, not reached in practical calculations. The following brief comments are related to our new approach, whose basic semi-discrete and discrete formulae (2.8) and (2.9) have been derived from conservation of momentum primarily.

(a) Conservation of mass: This can be expressed as $\mathrm{d}m=\mathrm{d}m_0$, $\varrho\mathrm{d}V=\varrho_0\mathrm{d}V_0$ for certain initial mass m_0, volume V_0 and density ϱ_0 and their values m, V and ϱ for the current (deformed) configuration. Thus, when e.g. decreasing the element volume, the density of the element must be increased proportionally.

(b) Conservation of energy: This is satisfied explicitly in the calculation of the impact of bodies using the presented algorithm because the magnitude of the opposite impact forces $\mathbf{f}_C$ and $\mathbf{f}_Q$, acting respectively on the points C and Q of the impacted bodies, have been calculated on the base of just this law.

(c) Conservation of momentum, in general by (2.1): This is satisfied implicitly, because the unknown contact force is introduced in the algorithm by the opposite forces acting on the impacted points, so the global momentum will not be influenced.

3.5. Calculation details. To support the reader-friendliness, the pseudo-code of Algorithm 2 represents the calculation scheme for contact pair as described above and is used for composition of $\mathbf{G}_s(\cdot,\cdot)$. Such scheme includes all impact phenomena on internal interfaces, discussed in Section 3. Both physical and geometrical non-linearities are handled by the reconfiguration of Ω_t, including related finite element mesh modifications, in equidistant discrete time steps t from 0 to τ.

Algorithm 2 Calculation of the nodal forces $\mathbf{f}_A$, $\mathbf{f}_B$ and $\mathbf{f}_C$.

Input: h, β, E, $\mathcal{A}_\eta$ of the corresponding ηth structural element at segment AB, $\mathbf{p}_I(0)$, $\mathbf{v}_I$, m_I with $I \in \{A, B, C\}$

Output: nodal forces $\mathbf{f}_A$, $\mathbf{f}_B$ and $\mathbf{f}_C$ as parts of the global vector $\mathbf{G}_s$

1: finding the point and time of impact of moving point into moving surface by Section 3.1 from its positions and velocities;
2: determination of the direction of impact forces $\mathbf{e}_C$ by Section 3.2 from its positions and velocities;
3: calculation of change of kinetic energy $\Delta\Pi_k(\mathbf{f}_C)$ by Section 3.3.2 from its masses and velocities (3.11);
4: calculation of change of potential elastic energy $\Delta\Pi_\sigma(\mathbf{f}_C)$ by Section 3.3.3 from its positions and material characteristics (3.12);
5: calculation of change of potential energy of position $\Delta\Pi_p(\mathbf{f}_C)$ by Section 3.3.4 from its masses and forces acting on its nodes (3.14);
6: calculation of the magnitude of impact nodal forces $\mathbf{f}_C$ from total energy change $\Delta\Pi = \Delta\Pi_k(\mathbf{f}_C) + \Delta\Pi_\sigma(\mathbf{f}_C) + \Delta\Pi_p(\mathbf{f}_C) = 0$ by Section 3.3.5;
7: calculation of the nodal forces $\mathbf{f}_A$, $\mathbf{f}_B$ from $\mathbf{f}_C$ by (3.20).

4. Illustrative examples

The validation of the algorithms described above was performed on the example of an elastic rod impacting a rigid segment, described in [32] generally. In our case, the rigid barrier is represented by a horizontal rigid segment with both nodes supported by Section 3. The input values were taken from [42], which will also serve for comparison of results.

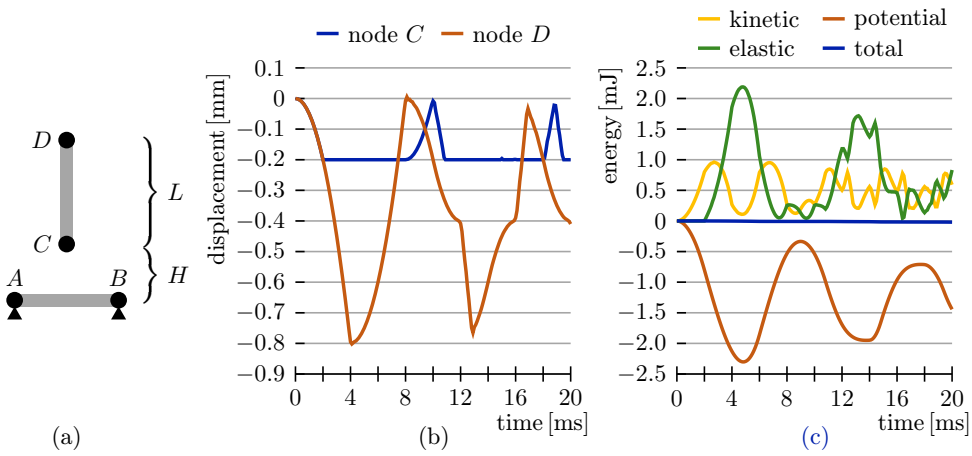

Figure 4. (a) An elastic rod impacting a rigid segment. (b) Displacements of the nodes C and D with $h = 10^{-8}$ s. (c) Decomposition of total energy to its kinetic, potential and elastic components corresponding to (b).

Fig. 4 (a) shows a model of a rod of total length $L = 2\,\mathrm{m}$, cross section area $\mathcal{A} = 10^{-5}\,\mathrm{m}^2$, Young modulus $E = 2000\,\mathrm{Pa}$ and mass density $\varrho = 2000\,\mathrm{kg/m}^3$, divided into 100 elements with its mass discretized to the nodes, which is released from the height $H = 0.0002\,\mathrm{m}$ under gravity $g = 100\,\mathrm{m/s}^2$ in the vertical direction towards a rigid segment AB. The calculation time step $h = 10^{-8}\,\mathrm{s}$ is applied. The friction parameter $\beta = 0$ is used. Fig. 4 (b) presents the time development of displacements of nodes C and D. The displacement of the nodes C and D corresponds to the analytical solution, presented in [42], as well. Fig. 4 (c) shows the changes of energy components in time, thus it can be seen as an indicator whether the energy conservation law is satisfied.

Let us now compare these results with the ones following from the penalty method introduced in [42]. This method depends on the parameter P defined in [42]. Fig. 5 shows the dependence of the results on P. We see that the results are correct for a sufficiently large value of P. However, its value is not a priori known. In addition, for too large values of P, significant rounding errors are observed as it is usual for penalty methods.

Fig. 5 shows the time development of displacements of nodes C and D and the changes of energy components in time. Only at a particular P, the displacement corresponds to the analytical solution and the energy is conserved during the impact.

Fig. 6 demonstrates analogous results for a slightly more general case: square truss structure with side length $a = 0.25\,\mathrm{m}$, cross section area $\mathcal{A} = 1\,\mathrm{m}^2$, Young modulus $E = 10^8\,\mathrm{Pa}$ and mass density $\varrho = 10^4\,\mathrm{kg/m}^3$, with its mass discretized to

the nodes, falling on a supported truss rod under gravity $g = 10\,\mathrm{m/s^2}$. The calculation time step $h = 10^{-6}\,\mathrm{s}$ is applied. Significantly different results correspond to zero (short contact point sliding along the rigid obstacle is observed) and absolute barrier friction (no contact point sliding) while the energy conservation law is satisfied in both cases.

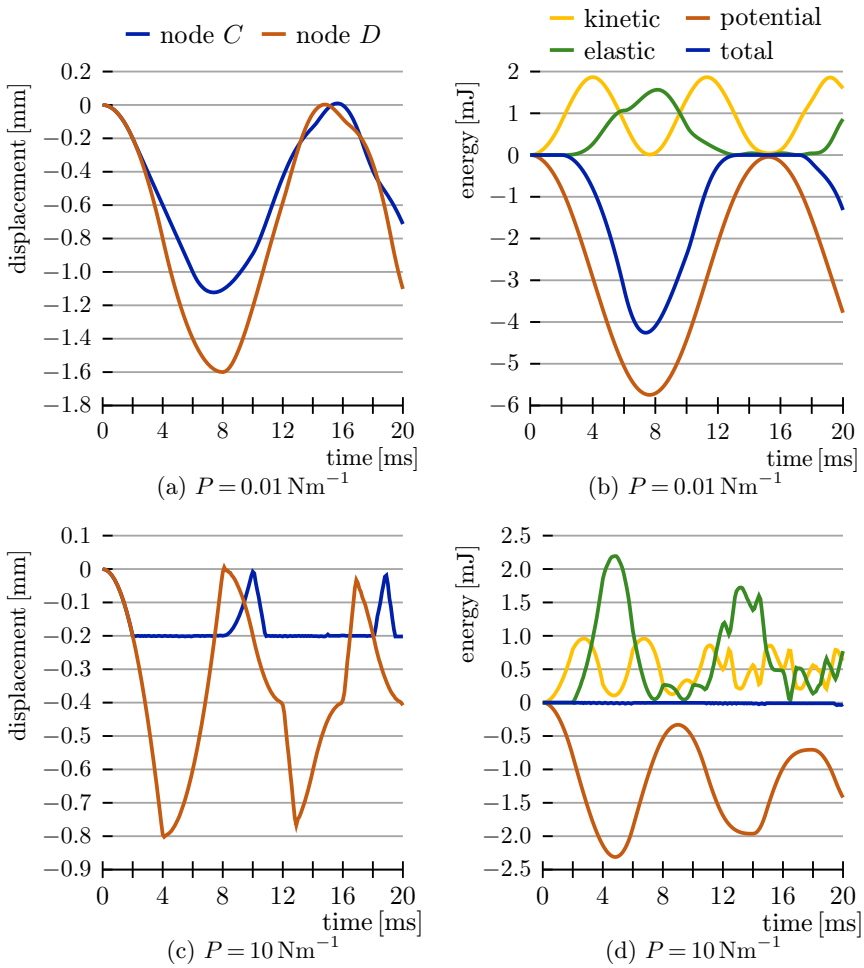

(a) $P = 0.01\,\mathrm{Nm^{-1}}$ (b) $P = 0.01\,\mathrm{Nm^{-1}}$

(c) $P = 10\,\mathrm{Nm^{-1}}$ (d) $P = 10\,\mathrm{Nm^{-1}}$

Figure 5. Left part of the figure shows displacements of the nodes C and D with $h = 10^{-8}\,\mathrm{s}$ and right part decomposition of total energy, both calculated by the penalty method.

Frictionless results obtained by the presented algorithm are compared with the penalty method again with various values of the penalty stiffness P; this is documented by Fig. 7. The energy conservation law during the impact is satisfied only at certain P.

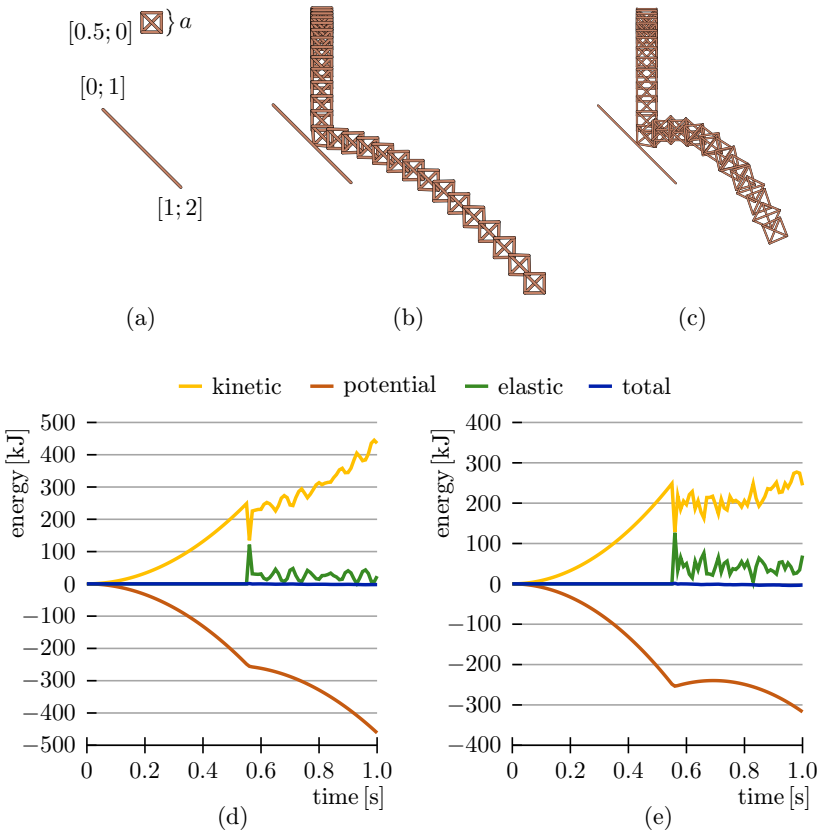

Figure 6. (a) Square truss structure impacting a supported truss rod. Phases of the bounce with (b) zero friction, (c) absolute friction; the decomposition of total energy for (d) zero and (e) absolute friction.

5. Conclusions

The paper has introduced a physically correct and computationally efficient algorithm for contact/impact of bodies. This algorithm was implemented by the authors in a test computer program and its correctness and efficiency was proved by numerous numerical examples, where all the energy components were monitored. It was shown that during each impact, the conservation of energy is satisfied perfectly, in addition to the implicit exact conservation of momentum.

The numerical tests have also shown the conditional stability of the presented algorithm. The principal ideas of the algorithm, presented and implemented in $\mathbb{R}^2$ for simplicity, can be extended to $\mathbb{R}^3$, too, as the next phase of this research. The advantages of the new algorithm can be seen at least in comparison with the penalty method, widely used in other computer programs.

The main advantage of the new algorithm is exact fulfilling of the energy conservation during collisions of bodies. In contrast to the penalty method, where the energy conservation is not satisfied exactly but is dependent on the chosen contact stiffness, the presented algorithm exactly fulfils the energy conservation law generally with no dependence on any selectable parameter. The algorithm can also take into account the possible energy dissipation and friction between bodies during impact easily.

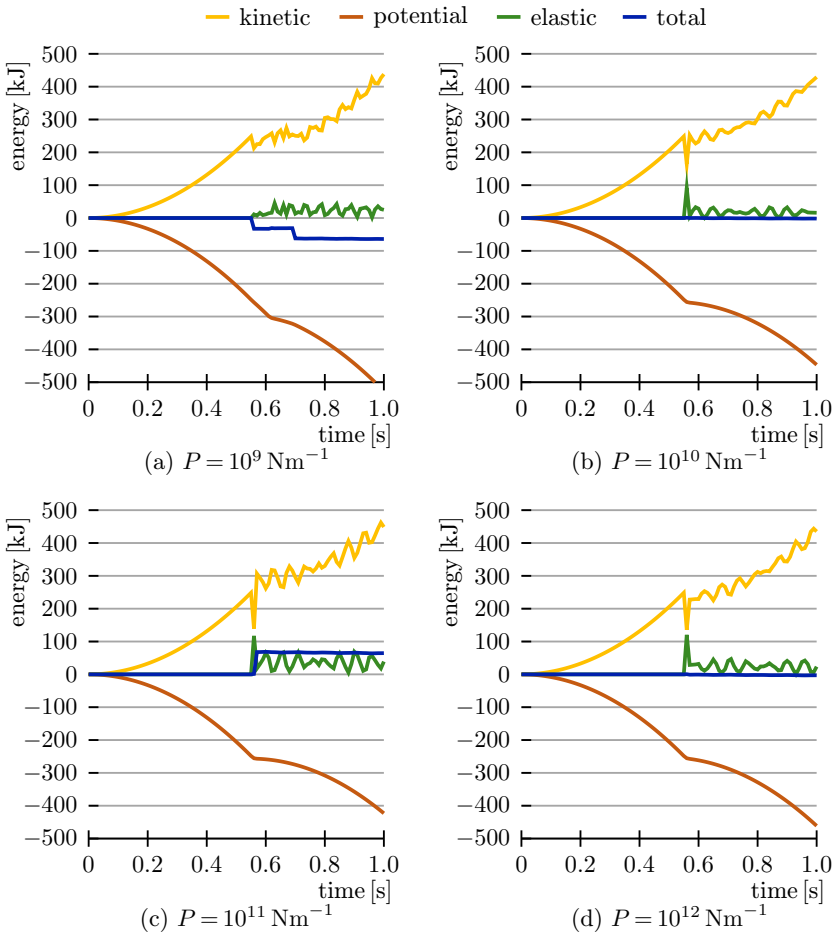

Figure 7. Decomposition of the total energy obtained by the penalty method.

The quantification of the time of calculation under comparable conditions shows that the performance of the new algorithm is slightly higher than that of the penalty method. The numerical solution of the non-linear equation (3.16) converges very quickly, in most cases only two or three iterations are needed, independently of the

problem size. The implementation of the presented algorithm for collision analysis of bodies into the widely used commercial software package RFEM for finite element structural analysis is under development.

Appendix A. Stability of an explicit computational scheme

Respecting all notations introduced by Section 2, let us notice that $\mathbf{M}$ and $\mathbf{F}_s$ in (2.9) can be seen as proportional to δ^2, unlike $\mathbf{C}$ and $\mathbf{K}$, proportional to δ, thanks to the derivatives $\varphi_{ip,j}$ and $\varphi_{kp,l}$ by (2.7), as evident from (2.4), and unlike $\mathbf{G}_s(\mathbf{u}_s)$, too, proportional to δ because of the presence of surface integrals. The obvious remedy is to introduce $\overline{\mathbf{C}} = \mathbf{C}\delta^2$, $\overline{\mathbf{K}} = \mathbf{K}\delta^2$ and $\overline{\mathbf{G}}_s(\mathbf{u}_s, \mathbf{v}_s) = \mathbf{G}_s(\mathbf{u}_s, \mathbf{v}_s)\delta$. Consequently, (2.9) implies

$$\Big(\mathbf{M} - \frac{h}{\delta^2}\overline{\mathbf{C}}\Big)(\mathbf{v}_{s+1/2} - \mathbf{v}_{s-1/2}) + \frac{h}{\delta^2}(\overline{\mathbf{C}} - h\overline{\mathbf{K}})\mathbf{v}_{s+1/2} + \frac{h}{\delta^2}\overline{\mathbf{K}}\mathbf{u}_{s+1} = h\mathbf{F}_s + \frac{h}{\delta}\overline{\mathbf{G}}_s(\mathbf{u}_s, \mathbf{v}_s). \tag{A.1}$$

Multiplying (A.1) by $\mathbf{v}_{s+1/2}$ from the left and summing the result up with $s \in \{1, \dots, r\}$, where $r \in \{1, \dots, m+1\}$, we obtain

$$\begin{aligned}
&\frac{1}{2}\mathbf{v}_{r+1/2}^\top\Big(\mathbf{M} - \frac{h}{\delta^2}\overline{\mathbf{C}}\Big)\mathbf{v}_{r+1/2} + \frac{1}{2}\sum_{s=0}^{r}(\mathbf{u}_{s+1} - \mathbf{u}_s)^\top\overline{\mathbf{K}}(\mathbf{u}_{s+1} - \mathbf{u}_s) \\
&\qquad + \frac{1}{2}\sum_{s=0}^{r}(\mathbf{v}_{s+1/2} - \mathbf{v}_{s-1/2})^\top\Big(\mathbf{M} - \frac{h}{\delta^2}\overline{\mathbf{C}}\Big)(\mathbf{v}_{s+1/2} - \mathbf{v}_{s-1/2}) \\
&\qquad + \frac{h}{\delta^2}\sum_{s=0}^{r}\mathbf{v}_{s+1/2}^\top\Big(\overline{\mathbf{C}} - \frac{h}{2}\overline{\mathbf{K}}\Big)\mathbf{v}_{s+1/2} + \frac{1}{\delta^2}\mathbf{u}_{r+1}^\top\overline{\mathbf{K}}\mathbf{u}_{r+1} \\
&= h\sum_{s=0}^{r}\mathbf{v}_{s+1/2}^\top\mathbf{F}_s + \frac{h}{\delta}\sum_{s=1}^{r}\mathbf{v}_{s+1/2}^\top\overline{\mathbf{G}}_s(\mathbf{u}_s, \mathbf{v}_s) \\
&\qquad + \frac{1}{2}\mathbf{v}_{-1/2}^\top\Big(\mathbf{M} - \frac{h}{\delta^2}\overline{\mathbf{C}}\Big)\mathbf{v}_{-1/2}.
\end{aligned} \tag{A.2}$$

Thanks to the positive definiteness of $\mathbf{M}$, $\overline{\mathbf{C}}$ and $\overline{\mathbf{K}}$, all 4 left-hand-side additive terms of (A.2) can be made always positive for sufficiently small h and certain $h \leqslant \mathfrak{C}\delta^2$; an easy evaluation of a positive constant $\mathfrak{C}$ is not available in general. Moreover, the 1st such term admits its lower bound (a) $\mathfrak{C}_0|v_{r+1/2}|^2$ for a positive constant $\mathfrak{C}_0$, as well as the 3rd such term its lower bound (b) $\mathfrak{C}_0\sum_{s=1}^{r}|v_{s+1/2}|^2$ and the 4th one its lower bound (c) $(\mathfrak{C}_0/\delta_0^2)|u_{r+1}|^2$ assuming $\delta \geqslant \delta_0$ for a positive constant δ_0; $|\cdot|$ here

denotes the Euclidean norm in $\mathbb{R}^N$. The last right-hand-side additive term can be bounded by another positive constant, thanks to the above introduced setting of $\mathbf{v}_{-1/2}$. The 1st such term can be estimated, using the Cauchy-Schwarz inequality, for an arbitrary positive ε as

$$h\sum_{s=0}^{r}\mathbf{v}_{s+1/2}^{\top}\mathbf{F}_s \leqslant h\sum_{s=0}^{r}|\mathbf{v}_{s+1/2}|\,|\mathbf{F}_s| \leqslant \frac{\varepsilon h}{2}\sum_{s=0}^{r}|\mathbf{v}_{s+1/2}|^2 + \frac{h}{2\varepsilon}\sum_{s=0}^{r}|\mathbf{F}_s|^2, \tag{A.3}$$

the 2nd one then similarly as

$$\begin{aligned}\frac{h}{\delta}\sum_{s=0}^{r}\mathbf{v}_{s+1/2}^{\top}\mathbf{G}_s(\mathbf{u}_s,\mathbf{v}_s) &\leqslant \frac{h\overline{\gamma}}{\delta}\sum_{s=0}^{r}|\mathbf{v}_{s+1/2}|(|\mathbf{u}_s|+|\mathbf{v}_s|)\\ &\leqslant \frac{\varepsilon h}{2\delta^2}\sum_{s=1}^{r}|\mathbf{v}_{s+1/2}|^2 + \frac{h\overline{\gamma}}{\varepsilon}\sum_{s=0}^{r}|\mathbf{u}_s|^2 + \frac{h\overline{\gamma}}{\varepsilon}\sum_{s=0}^{r}|\mathbf{v}_s|^2.\end{aligned} \tag{A.4}$$

The upper boundedness of the 2nd right-hand-side additive terms of both (A.3) and (A.4) is evident. The 1st such terms of (A.3) and (A.4) can vanish due to (a) and (b), respectively, as well as the last such term of (A.4), because (2.9) implies $2|\mathbf{v}_s|^2 = \frac{1}{2}|\mathbf{v}_{s-1/2}+\mathbf{v}_{s+1/2}|^2 \leqslant |\mathbf{v}_{s-1/2}|^2 + |\mathbf{v}_{s-1/2}|^2$; for the 3rd one of (A.4), supported by c), corresponding to non-linear contact phenomena, such direct approach is not available. However, from all preceding estimates we can summarize $|v_{r+1/2}|^2 \leqslant \overline{\mathfrak{C}}\Big(1+\sum_{s=1}^{r}|v_{s+1/2}|^2\Big)$ with certain positive constant $\overline{\mathfrak{C}}$, therefore the discrete version of the Gronwall lemma gives the required boundedness of $|v_{r+1/2}|$.

References

[1] *K. Abe, N. Higashimori, M. Kubo, H. Fujiwara, Y. Iso*: A remark on the Courant-Friedrichs-Lewy condition in finite difference approach to PDE's. Adv. Appl. Math. Mech. *6* (2014), 693–698. MR doi

[2] *M. Ahmad, K. A. Ismail, F. Mat*: Impact models and coefficient of restitution: A review. ARPN J. Eng. Appl. Sci. *11* (2016), 6549–6555.

[3] *R. E. Bank, T. Dupont*: An optimal order process for solving finite element equations. Math. Comput. *36* (1981), 35–51. zbl MR doi

[4] *K.-J. Bathe*: Finite Element Procedures. Prentice Hall, New Jersey, 2009.

[5] *A. Bermúdez de Castro*: Continuum Thermomechanics. Progress in Mathematical Physics 43. Birkhäuser, Basel, 2005. zbl MR doi

[6] *S. C. Brenner, L. R. Scott*:, Texts in Applied Mathematics 15. Springer, New York (2002) The Mathematical Theory of Finite Element Methods. zbl MR doi

[7] *R. Courant, K. Friedrichs, H. Lewy*: Über die partiellen Differenzengleichungen der mathematischen Physik. Math. Ann. *100* (1928), 32–74. (In German.) zbl MR doi

[8] *C. Duriez, C. Andriot, A. Kheddar*: Signorini's contact model for deformable objects in haptic simulations. International Conference on Intelligent Robots and Systems (IROS). IEEE, Piscataway, 2004, pp. 3232–3237. doi

[9] *G. Duvaut, J. L. Lions*: Inequalities in Mechanics and Physics. Grundlehren der mathematischen Wissenschaften 219. Springer, Berlin, 1976. zbl MR doi
[10] *C. Eck, J. Jarušek, M. Sofonea*: A dynamic elastic-visco-plastic unilateral contact problems with normal damped response and Coulomb friction. Eur. J. Appl. Math. *21* (2010), 229–251. zbl MR doi
[11] *A. Francavilla, O. C. Zienkiewicz*: A note on numerical computation of elastic contact problems. Int. J. Numer. Methods Eng. *9* (1975), 913–924. doi
[12] *J. O. Halquist* (ed.): LS-DYNA Theoretical Manual. Livermore Software Technology Corporation, Livermore, 2006.
[13] *J. O. Halquist, G. Goudreau, D. J. Benson*: Sliding interfaces with contact-impact in large-scale Lagrangian computations. Comput. Methods Appl. Mech. Eng. *51* (1985), 107–137. zbl MR doi
[14] *J. Han, H. Zeng*: Variational analysis and optimal control of dynamic unilateral contact models with friction. J. Math. Anal. Appl. *473* (2019), 712–748. zbl MR doi
[15] *K. Hashiguchi*: Elastoplasticity Theory. Lecture Notes in Applied and Computational Mechanics 69. Springer, Berlin, 2014. zbl MR doi
[16] *T. J. R. Hughes, R. L. Taylor, W. Kanoknukulchai*: A finite element method for large displacement contact and impact problems. Formulations and Computational Algorithms in Finite Element Analysis. M.I.T. Press, Cambridge, 1977, pp. 468–495. MR
[17] *G. Kloosterman, R. M. J. van Damme, A. H. van der Boogaard, J. Huétink*: A geometrical-based contact algorithm using a barrier method. Int. J. Numer. Methods Eng. *51* (2001), 865–882. zbl MR doi
[18] *G. K. Kocur, Y. E. Harmanci, E. Chatzi, H. Steeb, B. Markert*: Automated identification of the coefficient of restitution via bouncing ball measurement. Arch. Appl. Mech. *91* (2021), 47–60. doi
[19] *T. A. Laursen*: Computational Contact and Impact Mechanics: Fundamentals of Modeling Interfacial Phenomena in Nonlinear Finite Element Analysis. Springer, Berlin, 2002. zbl MR doi
[20] *J. Li, K. Yu, X. Li*: A novel family of controllably dissipative composite integration algorithms for structural dynamic analysis. Nonlinear Dyn. *96* (2019), 2475–2507. doi
[21] *J.-L. Lions*: Quelques méthodes de résolution des problèmes aux limites non linéaires. Dunod, Paris, 1969. (In French.) zbl MR
[22] *Y. F. Liu, J. Li, Z. M. Zhang, X. H. Hu, W. J. Zhang*: Experimental comparison of five friction models on the same test-bed of the micro stick-slip motion system. Mech. Sci. *6* (2015), 15–28. doi
[23] *J. Na, Q. Chen, X. Ren*: Adaptive Identification and Control of Uncertain Systems with Non-Smooth Dynamics. Emerging Methodologies and Applications in Modelling, Identification and Control. Academic Press, Amsterdam, 2018. zbl doi
[24] *I. Němec, H. Štekbauer, A. Vaněčková, Z. Vlk*: Explicit and implicit method in nonlinear seismic analysis. Dynamics of Civil Engineering and Transport Structures and Wind Engineering – DYN-WIND'2017. MATEC Web of Conferences 107. EDP Sciences, Paris, 2017, pp. Article ID 66, 8 pages. doi
[25] *M. A. Puso*: A 3D mortar method for solid mechanics. Int. J. Numer. Methods Eng. *59* (2004), 315–336. zbl doi
[26] *V. Rek, J. Vala*: On a distributed computing platform for a class of contact-impact problems. Seminar on Numerical Analysis (SNA'21). Institute of Geonics CAS, Ostrava, 2021, pp. 64–67.
[27] *K. Rektorys*: The Method of Discretization in Time and Partial Differential Equations. Mathematics and Its Applications (East European Series) 4. D. Reidel, Dordrecht, 1982. zbl MR

[28] *T. Roubíček*: Nonlinear Partial Differential Equations with Applications. ISNM. International Series of Numerical Mathematics 153. Birkhäuser, Basel, 2005. zbl MR doi
[29] *J. M. Sanz-Serna, M. N. Spijker*: Regions of stability, equivalence theorems and the Courant-Friedrichs-Lewy condition. Numer. Math. *49* (1986), 319–329. zbl MR doi
[30] *A. L. Schwab*: On the interpretation of the Lagrange multipliers in the constraint formulation of contact problems; or why are some multipliers always zero? Proc. ASME International Design Engineering Technical Conferences & Computers and Information in Engineering Conference IDETC/CIE. ASME, New York, 2014, pp. 1–5.
[31] *F. Sewerin, P. Papadopoulos*: On the finite element solution of frictionless contact problems using an exact penalty approach. Comput. Methods Appl. Mech. Eng. *368* (2020), Article ID 113108, 24 pages. zbl MR doi
[32] *P. Shi*: The restitution coefficient for a linear elastic rod. Math. Comput. Modelling *28* (1998), 427–435. zbl MR doi
[33] *M. Sofonea, D. Danan, C. Zheng*: Primal and dual variational formulation of frictional contact problem. Mediterr. J. Math. *13* (2016), 857–872. zbl MR doi
[34] *H. Štekbauer*: The pulley element. Trans. VŠB-TU Ostrava *16* (2016), 161–164. doi
[35] *H. Štekbauer, R. Lang, M. Zeiner, D. Burkart*: A correct and efficient algorithm for impacts of bodies. Seminar on Numerical Analysis (SNA'21). Institute of Geonics CAS, Ostrava, 2021, pp. 55–58.
[36] *H. Štekbauer, I. Němec*: Modeling of welded connections using Lagrange multipliers. AIP Conf. Proc. *2293* (2020), Article ID 340013, 4 pages. doi
[37] *H. Štekbauer, Z. Vlk*: The modification of a node-to-node algorithm for the modelling of beam connections in RFEM and SCIA using the explicit method. Dynamics of Civil Engineering and Transport Structures and Wind Engineering – DYN-WIND'2017. MATEC Web of Conferences 107. EDP Sciences, Paris, 2017, pp. Article ID 60, 6 pages. doi
[38] *J. Vala, V. Kozák*: Computational analysis of quasi-brittle fracture in fibre reinforced cementitious composites. Theor. Appl. Fracture Mech. *107* (2020), Article ID 102486, 8 pages. doi
[39] *J. Vala, V. Kozák*: Non-local damage modelling of quasi-brittle composites. Appl. Math., Praha *66* (2021), 815–836. zbl MR doi
[40] *R. Weyler, J. Oliver, T. Sain, J. C. Cante*: On the contact domain method: A comparison of penalty and Lagrange multiplier implementations. Comput. Methods Appl. Mech. Eng. *205-208* (2012), 68–82. zbl MR doi
[41] *P. Wriggers*: Finite element algorithms for contact problems. Arch. Comput. Methods Eng. *2* (1995), 1–49. MR doi
[42] *S. R. Wu*: A variational principle for dynamic contact with large deformation. Comput. Methods Appl. Mech. Eng. *198* (2009), 2009–2015. zbl doi
[43] *S. R. Wu*: Corrigendum to: "A variational principle for dynamic contact with large deformation". Comput. Methods Appl. Mech. Eng. *199* (2009), 220. zbl doi
[44] *D. Xu, K. D. Hjelmstad*: A new node-to-node approach to contact/impact problems for two dimensional elastic solids subject to finite deformation. Newmark Structural Laboratory Report Series. University of Illinois, Urbana-Champaign, 2008; Available at `http://hdl.handle.net/2142/5318`.
[45] *B. Yang, T. A. Laursen*: A large deformation mortar formulation of self contact with finite sliding. Comput. Methods Appl. Mech. Eng. *197* (2008), 756–772. zbl MR doi
[46] *B. Yang, T. A. Laursen, X. Meng*: Two dimensional mortar contact methods for large deformation frictional sliding. Int. J. Numer. Methods Eng. *62* (2005), 1183–1225. zbl MR doi
[47] *V. A. Yastrebov*: Numerical Methods in Contact Mechanics. J. Wiley & Sons, London, 2013. zbl doi

[48] *G. Zavarise, L. de Lorenzis*: A modified node-to-segment algorithm passing the contact patch test. Int. J. Numer. Methods Eng. *79* (2009), 379–416. zbl doi
[49] *Z.-H. Zhong*: Finite Element Procedures for Contact-Impact Problems. Oxford University Press, Oxford, 1993.

Authors' address: *Hynek Štekbauer*, *Ivan Němec* (corresponding author), *Rostislav Lang*, *Daniel Burkart*, *Jiří Vala*, Brno University of Technology, Faculty of Civil Engineering, Institute of Structural Mechanics, Veveří 331/95, 602 00 Brno, Czech Republic, e-mail: `stekbauer.h@fce.vutbr.cz`, `nemec.i@fce.vutbr.cz`, `lang.r@fce.vutbr.cz`, `vala.j@fce.vutbr.cz`.